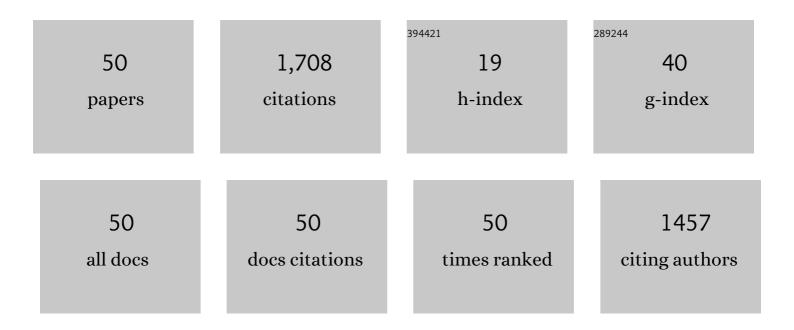
Toru Shinmei

List of Publications by Year in descending order

Source: https://exaly.com/author-pdf/9565374/publications.pdf Version: 2024-02-01



TODI SHINMEL

#	Article	IF	CITATIONS
1	Olivine-wadsleyite transition in the system (Mg,Fe)2SiO4. Journal of Geophysical Research, 2004, 109, .	3.3	272
2	Post-spinel transition in Mg2SiO4 determined by high P–T in situ X-ray diffractometry. Physics of the Earth and Planetary Interiors, 2003, 136, 11-24.	1.9	210
3	Iron Partitioning and Density Changes of Pyrolite in Earth's Lower Mantle. Science, 2010, 327, 193-195.	12.6	197
4	High-pressure transformations in MgAl2O4. Journal of Geophysical Research, 1998, 103, 20813-20818.	3.3	95
5	Effects of Water on the - Transformation Kinetics in San Carlos Olivine. , 1998, 281, 85-87.		93
6	Grain-growth kinetics in wadsleyite: Effects of chemical environment. Physics of the Earth and Planetary Interiors, 2006, 154, 30-43.	1.9	71
7	In situ X-ray diffraction study of enstatite up to 12 GPa and 1473 K and equations of state. American Mineralogist, 1999, 84, 1588-1594.	1.9	67
8	Experimental study on the stability of graphitic C3N4 under high pressure and high temperature. Diamond and Related Materials, 2011, 20, 819-825.	3.9	61
9	In situ X-ray observation of iron using Kawai-type apparatus equipped with sintered diamond: Absence of β phase up to 44 GPa and 2100 K. Geophysical Research Letters, 2003, 30, .	4.0	48
10	Spin transition of ferric iron in Al-bearing Mg–perovskite up to 200 GPa and its implication for the lower mantle. Earth and Planetary Science Letters, 2012, 317-318, 407-412.	4.4	47
11	Thermal equation of state of Mg3Al2Si3O12 pyrope garnet up to 19ÂGPa and 1,700ÂK. Physics and Chemistry of Minerals, 2012, 39, 589-598.	0.8	41
12	A novel large-volume Kawai-type apparatus and its application to the synthesis of sintered bodies of nano-polycrystalline diamond. Physics of the Earth and Planetary Interiors, 2014, 228, 255-261.	1.9	39
13	Phase relations in boron at pressures up to 18 GPa and temperatures up to 2200 <mml:math xmlns:mml="http://www.w3.org/1998/Math/MathML" display="inline"><mml:msup><mml:mrow /><mml:mo>â~</mml:mo></mml:mrow </mml:msup>C. Physical Review B, 2012, 85, .</mml:math 	3.2	32
14	Phase relations in the system MgSiO 3 –Al 2 O 3 up to 52 GPa and 2000 K. Physics of the Earth and Planetary Interiors, 2016, 257, 18-27.	1.9	31
15	Elasticity and sound velocities of polycrystalline Mg3Al2(SiO4)3 garnet up to 20 GPa and 1700 K. Journ of Applied Physics, 2012, 112, .	al _{2.5}	30
16	Effect of chemical environment on the hydrogen-related defect chemistry in wadsleyite. American Mineralogist, 2008, 93, 831-843.	1.9	27
17	Tough Hypoeutectic Zr-Based Bulk Metallic Glasses. Metallurgical and Materials Transactions A: Physical Metallurgy and Materials Science, 2011, 42, 1468-1475.	2.2	26
18	High-pressure rotational deformation apparatus to 135 GPa. Review of Scientific Instruments, 2017, 88, 044501.	1.3	25

TORU SHINMEI

#	Article	IF	CITATIONS
19	Polycrystalline Î ³ -boron: As hard as polycrystalline cubic boron nitride. Scripta Materialia, 2012, 67, 257-260.	5.2	23
20	Phase transition and compression behavior of phase D up to 46ÂGPa using multi-anvil apparatus with sintered diamond anvils. High Pressure Research, 2008, 28, 363-373.	1.2	21
21	A long-period superlattice phase in Mg97Zn1Yb2 alloys synthesized under high-pressure. Scripta Materialia, 2016, 121, 45-49.	5.2	17
22	Synthesis of coarse-grain-dispersed nano-polycrystalline cubic boron nitride by direct transformation under ultrahigh pressure. Diamond and Related Materials, 2017, 77, 25-34.	3.9	17
23	Cation order–disorder phase transitions in LiGaO2: Observation of the pathways of ternary wurtzite under high pressure. Journal of Applied Physics, 2010, 108, .	2.5	16
24	Disorder-activated Raman spectra of cubic rocksalt-type Li(1â^' <i>x</i>)/2Ga(1â^' <i>x</i>)/2 <i>Mx</i> O (<i>M</i> = Mg, Zn) alloys. Journal of Applied Physics, 2012, 112, .	2.5	16
25	Elastic wave velocity of polycrystalline Mj80Py20 garnet to 21ÂCPa and 2,000ÂK. Physics and Chemistry of Minerals, 2015, 42, 213-222.	0.8	16
26	Stability region of K0.2Na0.8AlSi3O8 hollandite at 22ÂGPa and 2273ÂK. Physics and Chemistry of Minerals, 2017, 44, 33-42.	0.8	16
27	Spin transition, substitution, and partitioning of iron in lower mantle minerals. Physics of the Earth and Planetary Interiors, 2014, 228, 186-191.	1.9	14
28	High-pressure, high-temperature plastic deformation of sintered diamonds. Diamond and Related Materials, 2015, 59, 95-103.	3.9	13
29	Synthesis of ultrafine nano-polycrystalline cubic boron nitride by direct transformation under ultrahigh pressure. Journal of the European Ceramic Society, 2018, 38, 2815-2822.	5.7	13
30	Density profiles of pyrolite and MORB compositions across the 660Âkm seismic discontinuity. High Pressure Research, 2008, 28, 335-349.	1.2	11
31	High pressure generation in Kawai-type multianvil apparatus using nano-polycrystalline diamond anvils. Comptes Rendus - Geoscience, 2019, 351, 260-268.	1.2	11
32	Synthesis of nano-polycrystalline diamond from glassy carbon at pressures up to 25â€GPa. High Pressure Research, 2020, 40, 96-106.	1.2	11
33	Generation of pressures to Â60 GPa in Kawai-type apparatus and stability of MnGeO3 perovskite at high pressure and high temperature. American Mineralogist, 2006, 91, 1342-1345.	1.9	9
34	High Pressure Experiments on Metalâ€Silicate Partitioning of Chlorine in a Magma Ocean: Implications for Terrestrial Chlorine Depletion. Geochemistry, Geophysics, Geosystems, 2017, 18, 3929-3945.	2.5	8
35	Garnets in the majorite–pyrope system: symmetry, lattice microstrain, and order–disorder of cations. Physics and Chemistry of Minerals, 2017, 44, 237-245.	0.8	8
36	Electronic properties of nano-polycrystalline diamond synthesised by high-pressure and high-temperature technique. Diamond and Related Materials, 2018, 84, 66-70.	3.9	8

#	Article	IF	CITATIONS
37	Phase Relations among D0 ₃ , α-Mg, and Long-Period Stacking Orders in Mg ₈₅ Zn ₆ Y ₉ Alloy under 3 GPa. Materials Transactions, 2015, 56, 910-913.	1.2	7
38	High nitrogen solubility in stishovite (SiO2) under lower mantle conditions. Scientific Reports, 2020, 10, 10897.	3.3	6
39	Nano-polycrystalline diamond synthesized from neutron-irradiated highly oriented pyrolytic graphite (HOPC). Diamond and Related Materials, 2018, 82, 132-136.	3.9	5
40	High-pressure and high-temperature synthesis of heavy lanthanide sesquisulfides Ln 2 S 3 (Ln =Yb and) Tj ETQq0	0 _{5.5} gBT /	Oyerlock 10
41	Halogen molecular modifications at high pressure: the case of iodine. Physical Chemistry Chemical Physics, 2021, 23, 3321-3326.	2.8	5
42	Benzo[<i>b</i>]trithiophene Polymer Network Prepared by Electrochemical Polymerization with a Combination of Thermal Conversion. Chemistry Letters, 2012, 41, 140-141.	1.3	4
43	Quenchable compressed graphite synthesized from neutron-irradiated highly oriented pyrolytic graphite in high pressure treatment at 1500 °C. Journal of Applied Physics, 2018, 123, 161577.	2.5	4
	Strength and plastic deformation of polycrystalline diamond composites. High Pressure Research,	1.0	

44	Strength and plastic deformation of polycrystalline diamond composites. High Pressure Research, 2020, 40, 35-53.	1.2	4
45	Interplay between local structure, vibrational and electronic properties on CuO under pressure. Physical Chemistry Chemical Physics, 2020, 22, 24299-24309.	2.8	3
46	Improvement of nano-polycrystalline diamond anvil cells with Zr-based bulk metallic glass cylinder for higher pressures: application to Laue-TOF diffractometer. High Pressure Research, 2022, 42, 121-135.	1.2	2
47	Pulsed laser irradiation as a process of conductive surface formation on nanopolycrystalline diamond. Japanese Journal of Applied Physics, 2018, 57, 118004.	1.5	1
48	Deep-ultraviolet near band-edge emissions from nano-polycrystalline diamond. High Pressure Research, 2020, 40, 140-147.	1.2	1
49	Mechanism of pressure induced amorphization of SnI4: A combined x-ray diffraction—x-ray absorption spectroscopy study. Journal of Chemical Physics, 2020, 153, 064501.	3.0	1
50	Dispersing InP Nanocrystals in Nano-polycrystalline Diamond during the Direct Conversion from Graphite. Materials Transactions, 2020, 61, 1707-1710.	1.2	0